Supporting Information

Effect of solution ions on the charge and performance of nanofiltration membranes

Rebecca S. Roth[1#], Liat Birnhack[1#], Mor Avidar[1], Elizabeth A. Hjelvik[2], Anthony P. Straub[2], and Razi Epsztein[1*]

[1]*Faculty of Civil and Environmental Engineering, Technion − Israel Institute of Technology, Haifa 32000, Israel*

[2]*Department of Civil, Environmental and Architectural Engineering, University of Colorado Boulder, Boulder, CO 80309-0428, USA*

Contents:

* Corresponding author: email: raziepsztein@technion.ac.il; Tel. +972 4 8293362

[#] These authors contributed equally to this work

Supplementary Notes

Speciation of weak acid systems

The extent of protonation of any weak acid system depends on the distance between the solution pH and the pK_a of the acid. To calculate the concentration of each species in a monoprotic acid system (such as carboxyl and amine acids), the following couple of equations are used[1]:

$$K_{\mathrm{a}} = \frac{(H^+)(A^-)}{(HA)} \quad (1)$$

$$A_{\mathrm{T}} = (A^-) + (HA) \quad (2)$$

where K_{a} is the thermodynamic equilibrium constant of the acid, (X) and [X] stand for the activity and concentration (mol L^{-1}) of X, respectively, and HA and A^- represent the acidic and basic species of the system, respectively. Note, that the acidic species of the carboxylic group is neutral, while the acidic species of the amine group is positively charged. Similarly, the basic species of the carboxyl and amine systems are negatively charged and neutral, respectively. A_T represents the sum of the weak acid system species, which remains constant with pH. For example, in our work, the sum of the concentrations of neutral and negatively charged carboxyl is denoted C_T (= [R-COOH] + [R-COO^-]) and the sum of amine species is denoted N_T (= [R-NH_2^+] + [R-NH]).

Using eq. 1 and 2, the concentration of each species can be expressed based on pH, K_{a} of the relevant acid, and A_T, (i.e., C_T for carboxyl and N_T for amine). Since equations 1 and 2 are general, and hold for any weak acid system, the expressions for the concentrations of A^- and HA of each weak acid differ only in the value of K_{a}. For example, the concentrations of neutral and negatively charged carboxyl, as a function of pH are computed using:

$$[\mathrm{R-COOH}] = \frac{(H^+)C_T}{K_{\mathrm{a}}+(H^+)} \quad (3)$$

$$[\mathrm{R-COO^-}] = \frac{K_{\mathrm{a}}C_{\mathrm{T}}}{K_{\mathrm{a}}+(H^+)} \quad (4)$$

Finally, x, the fraction of each species out of the total number of the relevant fixed group, is calculated using eq. 5-8, and shown on Supplementary Fig. 1a and b as a function of pH. Specifically, Supplementary Fig. 1a and b show that the protonation of each weak acid as a function of pH demonstrates the same trend and is most pronounced in the vicinity of the pK_{a} value where [HA] = [A^-] = 0.5A_T [1]. Additionally, the dashed line in Supplementary Fig. 1 shows that the fraction of negatively charged carboxyl at pH = pK_a -1 is less than 10%.

$$x_{\mathrm{R-COO^-}} = \frac{[\mathrm{R-COO^-}]}{C_{\mathrm{T}}} = \frac{K_{\mathrm{carboxyl}}}{K_{\mathrm{carboxyl}}+(H^+)} \quad (5)$$

$$x_{\mathrm{R-COOH}} = \frac{[\mathrm{R-COOH}]}{C_{\mathrm{T}}} \quad (6)$$

$$x_{\mathrm{R-NH_2^+}} = \frac{[\mathrm{R-NH_2^+}]}{N_\mathrm{T}} \quad (7)$$

$$x_{\mathrm{R-NH}} = \frac{[\mathrm{R-NH}]}{N_\mathrm{T}} \quad (8)$$

Buffer capacity of weak acid systems

Buffer capacity is the ability to resist changes in pH as a result of the addition of a strong acid or base. Weak acids (and bases) contribute to the buffer capacity, as they consume OH^- (and H^+) to form their conjugate bases (or acids). As a result, in case a strong acid or base is dosed to the solution, only a fraction of the protons (or hydroxides) will affect the pH value, and the shift in pH will be minor. Since buffer capacity of a solution is a superposition of the buffer capacities of each system that the solution contains[1], we deduce that the buffer capacity of the NF270 membrane is a superposition of the buffer capacity of its fixed carboxyl and amine groups. The two parameters that affect buffer capacity are the pH value and the total species concentration, A_T[2]. As A_T is higher, there are more species in the solution that can react with the protons and therefore curb the pH drop, and as a result the buffer capacity is higher. The pH value determines the species distribution (Supplementary Fig. 1a and b). In the context of buffer capacity, it is noted that for pH values far from the pK_a, one species concentration is negligible, and C_T practically consists only the other species. As a result, at pH > pK_a + 2 (or pH < pK_a - 2), any shift in the pH value due to addition of acid or base results in negligible changes in the concentration of the species (Supplementary Fig. 1a and b). Namely, the concentration of protons with which this species reacts is negligible. Conversely, for pH values that are close to the pK_a value, both species are dominant (i.e., at pK_a -1 < pH < pK_a + 1, both AH and A^- are dominant). Therefore, for pH value close to the pK_a, a change in the concentration of each of the species as a function of pH is significant, since their tendency to protonate or deprotonate is high. Consequently, in these pH ranges the buffer capacity is high, as shown in Supplementary Fig. 1c.

Calculations of concentrations near the membrane wall for computation of real rejection and permeability

In order to assess the real rejection and permeability, rather than the apparent ones, the effect of concentration polarization must be considered[3,4]. For this purpose, we evaluated the concentration near the membrane wall, C_m, using the thin film theory[5]. First, we calculated the Reynolds number, *Re*, to assess the flow regime. Since in our conditions, *Re* was calculated to be between 3300 and 5000 (for 20 and 40 ^oC, respectively) we focused on correlations based on turbulent flow. The value of C_m is evaluated by retrieving the mass transfer coefficient in the boundary layer, *k*, by the correlation for the Sherwood number in a rectangular channel without a spacer, using

$$Sh = 0.04Re^{0.75}Sc^{0.33} \quad (9)$$

where *Sh* is the Sherwood number ($Sh = k \cdot d_h/D$, where d_h is the hydraulic radius equal to $1.55 \cdot 10^{-3}$ m in our system, and *D* is the diffusion coefficient in water) and *Sc* is the Schmidt number ($Sc = \nu/D$ where n is the kinematic viscosity). The height and width of the flow channel in our system were 0.8 mm and 25 mm, respectively. The cell length was 0.06 m in our system. The diffusion coefficients of the different ions at the tested temperatures were calculated using the Stokes-Einstein equation using stokes radii at 25 ^{o}C (Supplementary Table 2). For each salt, the diffusion coefficient of the slower ion was used for the calculations of the Sherwood number. Finally, the calculated mass transfer coefficient was used to assess C_m using eq. 10.

$$C_m = (C_f - C_p)e^{J_w/k} + C_p \quad (10)$$

where *C* represents concentration (mol L^{-1}) and the subscripts m, f, and p represent the membrane wall, the feed and the permeate, and J_w is the water flux (m s^{-1}).

Assumptions behind the computation of salt permeability

The salt permeability was calculated based on the solution diffusion model. The model is developed based on the following assumptions:

1. The solution found in the bulk and inside the membrane (i.e., on both sides of the membrane and at the interface) is at equilibrium. That is, the chemical potential is constant. Therefore, there is no convection of fluid.
2. The pressure across the membrane is constant. As a result, the chemical potential changes across the membrane is only due to the change in activity.
3. Each constituent in the system is not influenced by any other constituent.

Evaluation of the pH near the membrane wall

There are six solutes present in the solutions during the filtration experiments that might affect the pH near the membrane wall: hydronium (H^+), hydroxide (OH^-), and unavoidably also species of the carbonate system (CO_2, H_2CO_3, HCO_3^- and CO_3^{-2}, out of which only the last two are ions). However, the solution used in the streaming potential experiments did not contain significant concentrations of the carbonate system species. Naturally, hydronium and hydroxide are present in all aqueous solutions, and play a significant role in determining the solution pH.

In our experiments these solutes had a negligible effect on the results, as explained hereinafter. Let us first discuss the potential influence of the uncharged species (i.e., $CO_{2(aq)}$ and $H_2CO_{3(aq)}$). Clearly, the permeability of the uncharged species is similar to that of water[5]; thus, their concentrations near the membrane wall remain similar to their feed bulk concentrations, and they will not cause a shift in pH. For this reason, the following explanation excludes the discussion on these two species. In addition, hydronium ion

permeates well through NF270[5] since it is small and its mobility in water is considerable. Thus, H^+ is also not expected to accumulate on the membrane wall and change the pH at the vicinity of the membrane. On the other hand, HCO_3^-, CO_3^{-2} and OH^- are rejected by the membrane and can accumulate in its vicinity. To better understand the potential influence of these species on the solution pH, Supplementary Table 3 shows their approximate concentrations in the feed solutions used in the filtration experiments. The concentrations were calculated based on the measured pH, the pK_a values of the carbonate system (i.e., 6.3 and 10.3) and considering that the feed solutions were not exposed to the atmosphere (i.e., closed system) and minimum exchange of atmospheric $CO_{2(g)}$ occurred. Different concentrations are listed in Supplementary Table 3 for each relevant figure shown in the main text.

To estimate the impact of rejection and concentration polarization on the pH near the membrane wall, it is acknowledged that HCO_3^- and CO_3^{-2} are weak bases that their accumulation can elevate the pH. To qualitatively evaluate this phenomenon, we divide the discussion on the potential influence of these species on the experimental results into two groups: (1) experiments conducted at pH between 7.0 and 7.5, where the membrane is highly negatively charged and far away from the pK_a of its groups; and (2) pH 4.0, which is close to the carboxylic pK_a. Regarding the first group of experiments, calculations show that even if the concentrations of the weak bases are doubled, the increase in pH is small (e.g., from 7.5 to 7.71, Supplementary Fig. 2). Additionally, the prime purpose of Figure 4 (in the main text) is to show the relationship between the trend of permeabilities and the trend of ZP. In other words, we show that ZP values are a good indicator for permeabilities. In this respect, in case the pH near the membrane is higher than the measured feed pH (i.e., above 7.5), the measured permeability should be compared with ZP measurements taken at pH > 7.5. However, ZP values are rather constant at pH > 7.5 (Fig. 3), thus, accumulation of OH^-, HCO_3^-, or CO_3^{-2} does not impact the main conclusion arising from the results shown in Fig 4.

Regarding the second group of experiments, in which the pH is below the pKa of the carboxylic groups (i.e., pH 4.0), calculations show that at these conditions, the concentrations of OH^-, HCO_3^-, or CO_3^{-2} are extremely low (Supplementary Table 3). In this case, considering that their concentration near the membrane wall may be doubled, the pH increase is below the detectable limit.

In summary, there are six species present in the feed of the permeability tests that may affect the pH. However, they do not affect the pH near the membrane wall either since their concentration is negligible or because they permeate the membrane freely, and do not accumulate. During the streaming potential experiments, $CO_{2(g)}$ was purged out, and therefore the pH was controlled solely by the dosage of acid and base.

<u>Minor effect of chloride adsorption on water permeability</u>

Water permeability was measured in the crossflow filtration system during the experiments that are detailed in the main text using eq. 5. In short, we sequentially elevated the temperature from 20 °C to 40 °C three times while keeping the ionic strength constant at 1 mM. Supplementary Fig. 3 shows that water permeability changed insignificantly (within the standard deviation) due to the exposure of the membrane to high temperature at the presence of salt, as there is no clear change in water permeability from the first run (from 20 ^{o}C to 40 ^{o}C) to the next two runs. This finding strengthens the conclusion that the clear decrease in salt permeability (Fig. 2c) resulting from the exposure to 40 ^{o}C is related to enhanced Donnan exclusion due to chloride adsorption to the membrane surface at elevated temperatures rather than structural changes of the polyamide.

Zeta potential measurement of four different salts

In order to examine the hypothesis that a more strongly hydrated ion is less attached to the membrane surface, the ζ of the NF270 membrane in contact with four single-salt solutions (LiCl, NaCl, KCl, and CsCl) was tested at pH values between ~2.0 and ~9.0. The four solutions were chloride-based salts of alkaline metals of gradually increased bare ion radius and decreased hydration enthalpy (Table 1), correlated to gradually elevated stickiness. The results imply that the tested cations are divided into two distinct groups, confirming that the more strongly hydrated ions (i.e., Li^+ and Na^+) are weakly attached to the membrane surface, resulting in a more negative ζ, while weakly hydrated and stickier ions (i.e., K^+ and Cs^+) better neutralize the membrane charge (Supplementary Fig 4). Since the differences between similar ions (e.g., Li^+ and Na^+ or K^+ and Cs^+) are minor, we chose to focus in the main text on comparing Li^+ and Cs^+ as they show more noticeable differences.

Chemical properties of membrane fixed groups

The NF270 membrane is manufactured via interfacial polymerization of piperazine (PIP) and trimesoyl chloride (TMC), resulting in the formation of carboxyl and amine fixed groups. To better understand the chemistry of these fixed groups, we evaluated their explicit structure, based on the known structure of the building blocks of the polyamide, i.e., PIP and TMC. The TMC is an aromatic ring that contains three acyl chloride groups. Possibly two acyl chloride groups can bond to the polymer chain and the third one can terminate the chain, and react in aqueous environment to form a carboxyl group. On the other hand, the aliphatic PIP contains two nitrogen atoms at opposite positions, enabling a bond to the polymer at one end, and a terminating amine group at the other end. The formed carboxyl and amine groups can react as weak acids (eq 1 and 2 in the main text, respectively, forming the species depicted in the 1st and 4th lines of Supplementary Table 1), of which the exact pK_a is depends on the chemistry of the R groups and the surrounding polymer. Thus, to evaluate the pK_a values we first considered the reported

thermodynamic pK_a values of the most analogous monomers. That is, substituting the R group of the carboxyl with an aromatic ring, resulting in a benzoic acid which is a close approximation of the structure of the group attached to the NF270 membrane (Supplementary Table 1). Similarly, N-benzoylpiperazine is the closest approximation of the structure of the amine group of the NF270 membrane, and thus the pK_a values of these acids were the basis of comparison for the evaluated pK_a values of the membrane.

Supplementary Figures

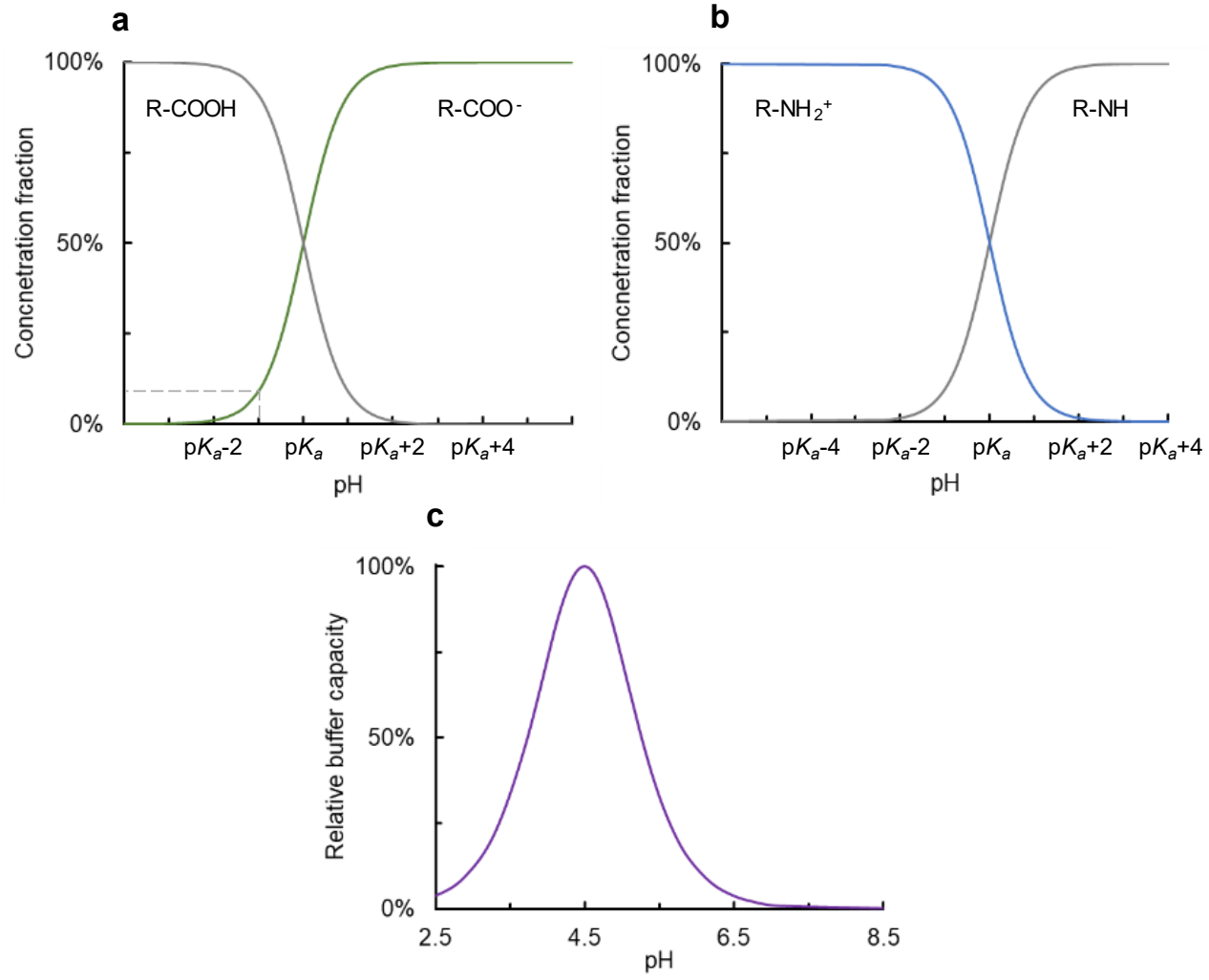

Supplementary Figure 1. **General representation of concentration fractions and buffer capacity of weak acid systems as a function of pH.** Distribution of the fraction of the species of (a) Carboxyl group (neutral R-COOH in gray and negatively charged R-COO^- in green) and (b) Amine (positively charged R-NH_2^+ in blue and neutral R-NH in green) as a function of pH and its distance from the pK_a. (c) Buffer capacity of monoprotic weak acid system.

File Edit Help

PrevPage | NextPage | NewPage | DeletePage | Copy | Paste

NAME:

TREATMENT PROCESS:		Initial	EqmAir	NaOH	NaHCO3
Unit:		Water	pp Atm	mg/l	mg/l
Purity of Process Chemical:				100.0%	100.0%
Amount:			0.00040	0.62	1.27
PARAMETERS (mostly mg/l)					
Temperature	C	25	25	25	25
Conductivity	mS/m	15	15	15	15
Total Dissolved Solids		100	100	101	101
Calcium, dissolved	Ca	0.0	0.0	0.0	0.0
pH		7.00	5.61	7.50	7.70
Alkalinity	CaCO3	0.00	0.00	0.78	1.53
Acidity	CaC03	0.00	1.62	0.85	1.60
Carbonic Species	CO2	0.00	0.71	0.71	1.38
CaCO3 PP	CaCO3	-13.5	-13.6	-13.1	-12.7

Page: 1

Supplementary Figure 2. Stasoft 4.0 screenshot demonstrating the theoretical calculation of the pH near the membrane wall for the conditions shown in Figure 4a in the main text. Water qualities from left to right: Initial water is distilled water. The second column simulates the water quality following equilibrium with atmospheric $CO_{2(g)}$. Next, is the bulk water following pH adjustment via NaOH dosage. Last, the water quality near the membrane wall, assuming the concentration of the main carbonate system species are doubled.

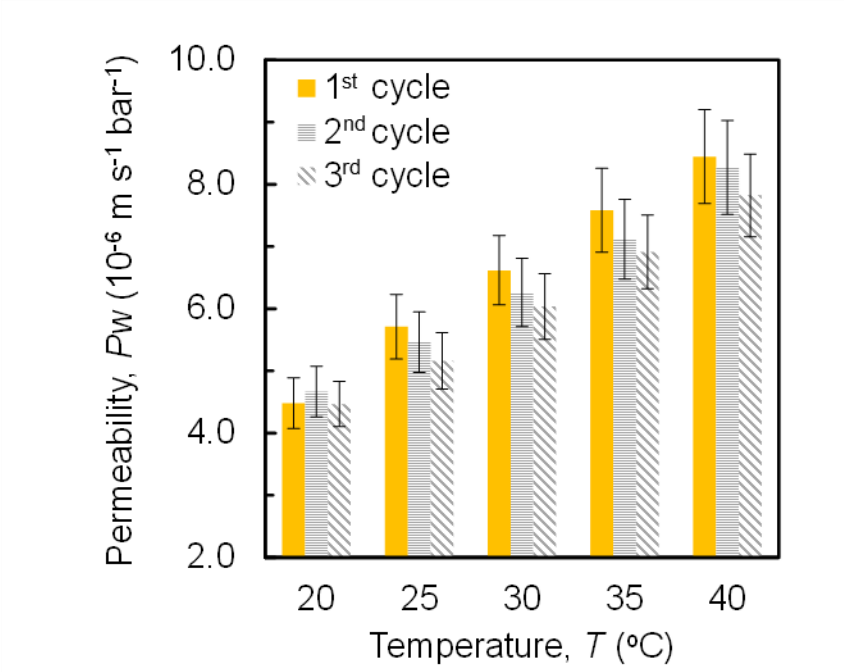

Supplementary Figure 3. **Water permeability during three consecutive experiments examining NaCl permeability as a function of temperature**. In each cycle, the temperature was elevated from 20 °C to 40 °C to explore chloride irreversible adsorption and its effect on Donnan exclusion. The same membrane coupons were used throughout the three experiments. Experimental conditions: 1 mM NaCl, applied pressure of 18 bar, and crossflow velocity of 2.13 m s^{-1}. Compaction of the membranes was conducted overnight at 20 bar and 20 ºC. Error bars represent standard deviation.

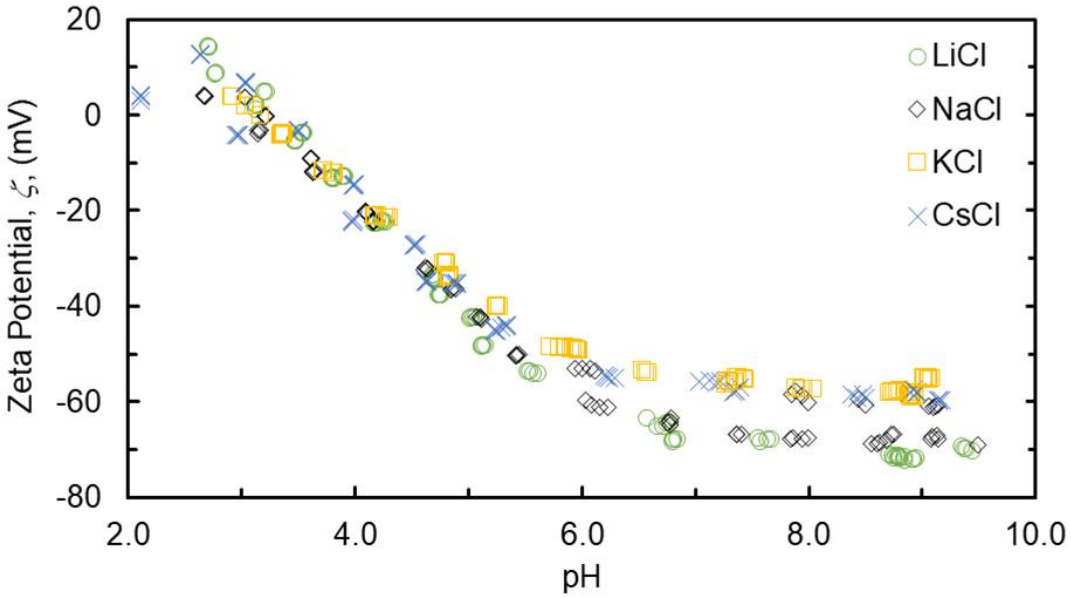

Supplementary Figure 4. Average (n=4) zeta potential, ζ, of the NF270 membrane as a function of pH using four single-salt solutions of 1 mM (LiCl, NaCl, KCl and CsCl) at 23 ± 0.8 °C.

Supplementary Tables

Supplementary Table 1. General and explicit representations of the carboxyl and amine groups at their protonated and deprotonated states.

		Acidic species	**Basic species**
Carboxyl acid system	General molecular formula	R-COOH	R-COO$^-$
	Molecular geometry of Benzoic, pK_a = 4.2	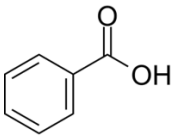	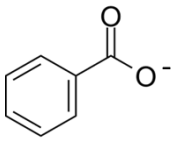
	Molecular geometry on the NF270 membrane polyamide	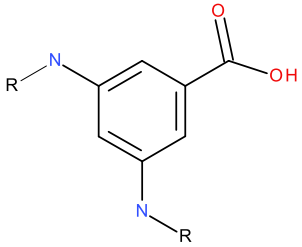	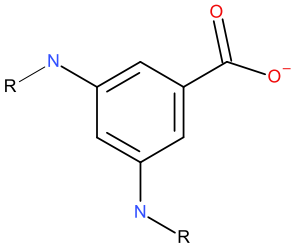
Amine acid system	General molecular formula	R-NH_2^+	R-NH
	Molecular geometry of N-benzoylpiperazine, pK_a = 8.48	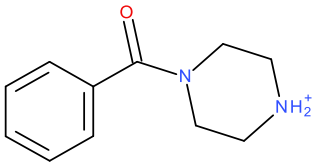	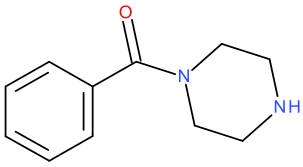
	Molecular geometry on the NF270 membrane polyamide	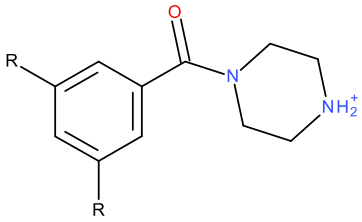	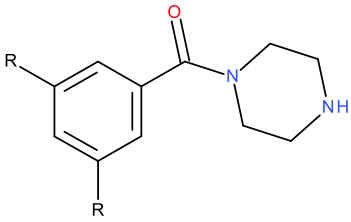

Supplementary Table 2. Stokes radius and diffusion coefficient at 25 °C of the tested ions that were used for evaluation of concentration polarization (for consistency, data was collected from the same source for a specific parameter, when possible). Also shown the mass transfer coefficient calculated for the different ions.

Ion	Stokes radius (Å) [6]	Diffusion coefficient, $D \times 10^9$ ($m^2\ s^{-1}$)	Mass transfer coefficient, $k \times 10^4$ ($m\ s^{-1}$)
Li^+	2.37	1.04	1.18
Na^+	1.84	1.17	1.40
Cs^+	1.19	2.06	1.87
Cl^-	1.21	2.03	1.85
H_3O^+	0.28	8.77	-
OH^-	0.46	5.34	-
HCO_3^-	2 – 2.2 [7]	1.19	-
CO_3^{-2}	2.66	0.92	-

Supplementary Table 3. Approximate concentrations (M) of ions in the solutions fed to the filtration system during the various experiments. $H_2CO_3^*$ represents the sum of $H_2CO_{3(aq)}$ and $CO_{2(aq)}$, as costomary[1].

Fig.	pH	Li^+	Cs^+	Na^+	Cl^-	H^+	OH^-	$H_2CO_3^*$	HCO_3^-	CO_3^{-2}
4a	4	10^{-3}	10^{-3}		10^{-3}	10^{-4}	10^{-10}	$1.8\cdot10^{-5}$	$8\cdot10^{-8}$	$3.9\cdot10^{-14}$
4a	7.5	10^{-3}	10^{-3}		10^{-3}	$10^{-7.5}$	$10^{-6.5}$	$1.2\cdot10^{-6}$	$1.7\cdot10^{-5}$	$2.5\cdot10^{-8}$
4a	7.5	$5\cdot10^{-2}$	$5\cdot10^{-2}$		10^{-3}	$10^{-7.5}$	$10^{-6.5}$	$8.2\cdot10^{-7}$	$1.6\cdot10^{-5}$	$4.3\cdot10^{-8}$
2c	7.0			10^{-3}	10^{-3}	10^{-7}	10^{-7}	$2.6\cdot10^{-6}$	$1.4\cdot10^{-5}$	$7.5\cdot10^{-9}$

Supplementary References

1. Lahav, O. & Birnhack, L. *Aquatic Chemistry*. *Aquatic Chemistry* (2019). doi:10.1515/9783110603958.

2. Birnhack, L., Voutchkov, N. & Lahav, O. Fundamental chemistry and engineering aspects of post-treatment processes for desalinated water-A review. *Desalination* vol. 273 Preprint at https://doi.org/10.1016/j.desal.2010.11.011 (2011).

3. Peer-Haim, O., Shefer, I., Singh, P., Nir, O. & Epsztein, R. The Adverse Effect of Concentration Polarization on Ion-Ion Selectivity in Nanofiltration. *Environ Sci Technol Lett* **10**, 363–371 (2023).

4. Song, L. & Elimelech, M. Theory of concentration polarization in crossflow filtration. *J. Chem. Soc., Faraday Trans.* **91**, 3389 (1995).

5. López, J. *et al.* Experimental and theoretical study of nanofiltration of weak electrolytes: SO42–/HSO4–/H+ system. *J Memb Sci* **550**, (2018).

6. Nightingale Jr, E. R. Phenomenological theory of ion solvation. Effective radii of hydrated ions. *J. Phys. Chem.* **63**, 1381–1387 (1959).

7. Hussain, A. *et al.* Ion Transport Behavior in Bipolar Membrane Electrodialysis: Role of Anions. *Ind Eng Chem Res* **62**, (2023).